OLED with Hole-Transporting Layer Fabricated by Ink-Jet Printing

F. Villani,[*1] *P. Vacca,*[1] *R. Miscioscia,*[1] *G. Nenna,*[1] *G. Burrasca,*[1] *T. Fasolino,*[1] *C. Minarini,*[1] *D. della Sala*[2]

Summary: we report about the fabrication of organic light-emitting diodes (OLEDs) ink-jet printing a hole-transporting polymer (PF6, poly(9,9-dihexyl-9H-fluorene-2,7-diyl)) on flexible substrate (PET) and performing the other layers through vacuum thermal evaporation. The aim of the work is to employ the ink-jet printing (IJP) technology, familiar as a method for printing on paper, in optoelectronic applications and to determine how the deposition method affects the functional material film properties and hence the ultimate device performances. In this line of work, ink-jet printed polymer films are compared to same spin-coated polymer from the electro-optical point of view: both prepared materials are adopted as HTLs of electroluminescent devices. All manufactured OLEDs are characterized and their behaviours are investigated and analyzed with theoretical models. The results show differences in current density and optical behaviours between the devices fabricated by means of the above mentioned technologies which can be justified in terms of different trap distribution induced by impurity energy levels associated to each process.

Keywords: electrical and optical properties; hole-transporting layers; ink-jet printing; OLED; polymer

Introduction

Ink-jet printing (IJP) provides a controllable method for selectively depositing solution-processed functional materials as thin films within well defined areas with a high degree of accuracy: small amounts of functional materials can be deposited by solution on defined surface areas and with the desired shape.[1–3] Thanks to this technology it is possible to perform material deposition and patterning at the same time. Moreover, the deposition does not need any employment of expensive masks and patterning does not require any chemical processes as photoresist activation and development, wet etching of undesired structures or other material subtraction-related treatments which can induce defects in functional organic layers. All this issues make this technology attractive for organic light-emitting diodes applications in comparison with the technologies conventionally employed in the organic material deposition (thermal evaporation in the case of small organic molecules, and spin-coating in the case of polymer materials). Indeed, IJP technology allows to overcome the traditional techniques limits related to large substrates coverage, solution wastage and lack of lateral patterning capability.[4–6] Thus, IJP assumes a key role in high resolution full-colour display applications thanks also to other remarkable advantages such as the lack of sensitivity to substrate defects being a contactless method, the applicability to several kinds of substrate including the flexible ones, the applicability to almost any

[1] Portici ENEA Research Center, Piazzale Enrico Fermi 1, 80055 Portici (NA), Italy
Fax: +39 0817723344;
E-mail: villani@portici.enea.it
[2] Casaccia ENEA Research Center, Via Anguillarese 301, 00123 S. Maria di Galeria (ROMA), Italy

low-viscosity liquid, and the reduction of production costs for both waste materials and number of process steps.[3]

The crucial element of IJP process is to keep the nozzles clear while the ultimate printed product has got some intrinsic limits due to the formation of rough films from joined drops and thickness not-uniformities due to drying process.[7,8] In relation to this last point, during this process the pinned droplet diameter remains constant and a solute transport towards the edges takes place because of the capillary fluid flow from the centre to the edge to replace the amount lost by evaporation. This phenomenon known as 'coffee-stain' effect can not be avoided and it causes a non-uniform material distribution which affects the optoelectronic device efficiency.

In order to understand how the deposition method influences OLED device performances we fabricated electroluminescent stacks in which the hole-transporting layer (HTL) is ink-jet printed or spin-coated employing the same solution, poly(9,9-dihexyl-9H-fluorene-2,7-diyl) (PF6) in toluene. The manufactured double-layer structures, with an electron-transporting layer (ETL) deposited on a hole-transporting layer, are those ones usually utilized to confine charges at the hetrojunction of the two semiconducting layers to improve the device performances. The fabricated ITO/PF6/tris 8-hydroxyquinoline aluminium salt (Alq_3)/Al structure, in which only PF6 polymer was deposited by two different technologies and all the other layers were performed by thermal evaporation, was not yet optimized for the highest efficiency but it was not essential for the purpose of our work. Electrical and optical OLEDs properties were investigated and analyzed with theoretical models available by literature.

Experimental Part

We fabricated double-layer OLEDs with bottom-emitting structure on flexible substrate: polymer substrate (PET)/transparent anode (ITO, indium tin oxide)/HTL/ETL/metallic cathode (Al, aluminium).

Commercial ITO-coated PET substrate was supplied by Diamond Coatings UK. More precisely, ITO was 6000 Å thick with a sheet resistance of 100 Ω/sq. The substrates were cleaned with deionised water, detergent and ultrasounds and dried in oven for 4 h at 50 °C. In order to define the OLED geometry we carried out the ITO patterning by conventional contact reverse photolithography.

Before ink-jet printing the polymer material, we treated the surface by a chemical wet process. A piranha solution, H_2SO_4:H_2O_2 4:1 (v/v), was performed to be used as oxidant treatment: the substrates were dipped in this solution for 5 min at room temperature. At the end of the piranha treatment, the ITO substrates were rinsed in distilled water and finally dried with nitrogen, immediately before the functional material deposition.

PF6 is a blue emitting polymer and it is soluble in common organic solvents. It was dissolved in a toluene solution (15 mg/ml) and ink-jet printed over the ITO to be employed as a hole-transporting material in the OLED structure. The ink-jet equipment has been especially designed by Aurel S.p.A. for printing functional materials on flexible substrates as reel or single sheet and non-flexible substrates. This printer uses piezoelectric Drop on Demand (DoD) technology and incorporates a Microdrop printhead with a 50 μm opening nozzle. In order to perform a continuous film by IJP technique, polymer solution was printed in the line shape on patterned substrate: sequences of overlapping droplets were printed at 1 Hz drop emission frequency and 200 μm/s printhead speed. IJP process was developed in environmental condition, at room temperature. Then, the printed material was baked in vacuum for 3 h at 60 °C.

PF6 films were also realized by spin-coating at 1000 rpm for 30 s from the same toluene solution. The spin-coating process was carried out using a Laurell Model WS-400B-6NPP spin coater in a class-100 clean

room environment. After the deposition, the spun films were baked at the same conditions of ink-jet printed material.

Alq_3, used as electron-transporting and emitting material, was deposited by thermal evaporation on both ink-jet printed and spin-coated polymer films. The deposition process was performed in high vacuum at a base pressure of 10^{-7} mbar. The layer thickness was 700 Å.

The aluminium cathode, 2000 Å thick, was evaporated as the final layer.

The active device area was 0.56 mm^2.

The contact angle measurements were performed by using a Dataphysics OCA 20 equipment at 21 °C and 50% relative humidity. We used water (polar) and diiodomethane (non polar) solvents to evaluate the polar and dispersion components of the surface energy. The standard error of contact angle measurements is $\pm$ 0.2°.

The film thickness was evaluated with a KLA Tencor P-10 surface profiler. The morphology was investigated by atomic force microscopy (AFM) with a Veeco Multimode Nanoscope V system. We measured the current-voltage (I-V) characteristics with a Keithley 2400 Power Supply SourceMeter® in voltage mode with constant increment steps and delay time of 1 s between each measurement point. We performed the electroluminescence (EL) measurements by using an integrating sphere and a calibrated photodiode (Newport 810UV) connected to a Keithley 6517A Electrometer. The OLED was put in a fixture in front of the integrating sphere window in such a way that only the light emitted in the forward direction was detected.

All the characterizations were performed in air at room temperature.

Results and Discussion

Figure 1 shows the optical micrograph of single and overlapping PF6 drops sequences on piranha-treated ITO/PET substrates.

The thickness of the drops ranged from 500 to 600 Å and the drops widths ranged from 300 to 320 μm. Piranha treatment effect was intended to improve the surface wettability. We understood this phenomenon comparing the print products on treated substrates with the drops ink-jet printed on untreated substrates. In this last case the drop thickness ranged from 950 to 1000 Å and, as we expected,[9] the drop widths were smaller than the corresponding values for treated substrates (250–260 μm).

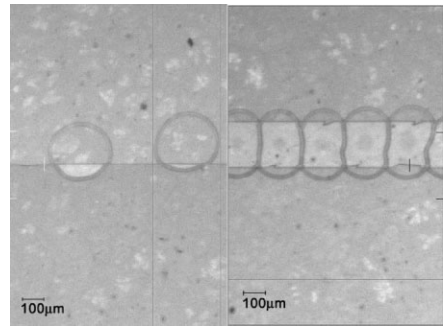

Figure 1.
Micrograph of single (on the left) and overlapping (on the right) PF6 IJ printed drop sequences on piranha-treated ITO/PET substrate.

The results obtained by surface profilometer analysis were confirmed by the surface energy investigations carried out by contact angle measurements. The measured surface energy for the PF6 solution ranged from 30 to 35 mJ/m^2, values comparable with surface energy of the untreated ITO/PET layer. The piranha etch solution, reacting with the substrate organics, increases the surface energy and reduces the contact angle, and hence increases the surface wettability.

On the other hand, all these issues affect drop surface roughness. Indeed, the smaller contact angle on treated substrate and hence also the thinner fluid layer at the droplet edge induce a non-uniform fast solvent evaporation. This fast diffusion of the polymer causes a roughness increase. We investigated this effect by AFM measurements. The average surface roughness of the IJ printed droplets on treated and untreated ITO/PET substrates were 1.55 nm and 0.39 nm, respectively. Anyway, even if the drops printed on piranha-treated

substrate exhibited a higher degree of roughness we choose this path to perform the HTL of OLED devices because the drops thickness and morphology represented a good trade-off in the manufacturing of functional OLED devices.

Figure 1 gives indications on the material distribution originated during drying process from the mass transport towards the dot edge and due to segregation as the solvent evaporated. A non-uniform film is produced in this way, with a large amount of polymer material preferentially distributed at the drop edges (darker areas), leaving the thinner central area (brighter areas) as functional area. In order to investigate the drop structure in details, we performed the surface profile analysis via AFM and pointed out that the drop central area thickness was around 150 Å, excluding small areas (far from dot edges) 600 Å thick (Figure 2).

Using these results as reference, we deposited by spin-coating 150 Å thick PF6 films on piranha-treated ITO/PET substrates. Alq_3 layer, 700 Å thick, and then aluminium cathode, 2000 Å thick, were grown on both IJ printed and spin-coated polymer films in the same evaporation run to complete the OLED structures. Vacuum was broken for all the devices between the Alq_3 deposition and the cathode evaporation for shadow-mask substitution.

The electro-optical behaviours of manufactured OLEDs were evaluated and analyzed. Current density-voltage characteristics of ITO/PF6/Alq_3/Al OLEDs are reported in Figure 3.

The electrical characteristics of fabricated devices had the same slope changes in log-log plots in three significant different zones, but slight differences resulted in each regime. This result pointed out that the device electrical properties were not strongly dependent from the deposition technique but it could induce some little modifications.

Observing Figure 3, the slope of J-V plot for the spin-coated device is smaller than the IJ printed one, not only because the non-uniform IJ drop thickness creates

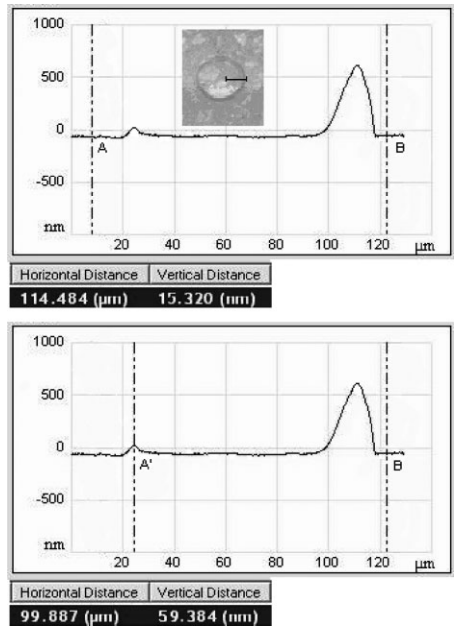

Figure 2.
Surface profile analysis via AFM scanning about half PF6 drop IJ printed on piranha-treated ITO/PET substrate (linear scanning 130 µm). The vertical distance is the surface profile measurement in different points of the drop (labelled by A, A′) respect to the external level (the substrate) (B); the horizontal distance is the measurement of the linear dimension A/A′-B. AFM scan was performed along the pointed out line in the insert image.

preferential conducting paths for the current flow across thinner area sections where the resistance is lower, but probably also because of the presence of different impurity levels that lead to a different traps distribution. More in detail, observing the J-V plots at higher fields, the current density behaviours can be approximated by the TCLC (Trap Charge Limited Current)[10,11]:

$$J = q\mu N_v \left(\frac{\varepsilon_r \varepsilon_0}{qN_t}\right)^m \frac{V^{m+1}}{d^{2m+1}} \quad (1)$$

where q is the electron charge, μ is the hole mobility, N_v is the state density in valence band and N_t is the total concentration of traps in the bandgap.[10]

In Figure 3, the exponent m can be evaluated as the slope of current density in

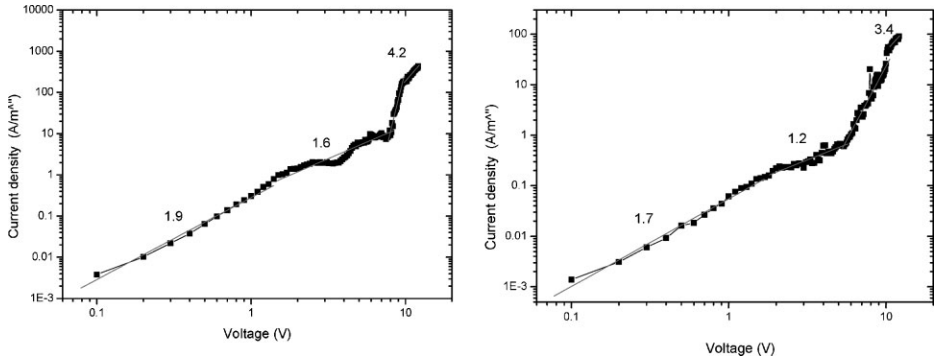

Figure 3.
The J-V log-log plot of the device with IJ-printed PF6, on the left; the corresponding spin-coated one, on the right.

a log-log plot. As we referred to the TCLC approximation (1), in this region $m+1>2$.

The relationship between m and trap energy level is quantified by the formula[10]:

$$m = \frac{E_t}{kT} \tag{2}$$

where E_t is the trap energy width, $k = 8{,}617^{*}10^{-5}$ (eV/K) is the Boltzmann constant and T is the absolute temperature. If we report our assumption at room temperature $T = 300\,K$, for IJP device $E_t = 83\,meV$ while the spin-coated device has $E_t = 62\,meV$. Thus, a broader distribution of trap energy levels can be associated to IJP process leading to higher currents density slopes and strong dependencies from electric field. These differences in current density behaviours can be justified by different impurity levels associated to each process.

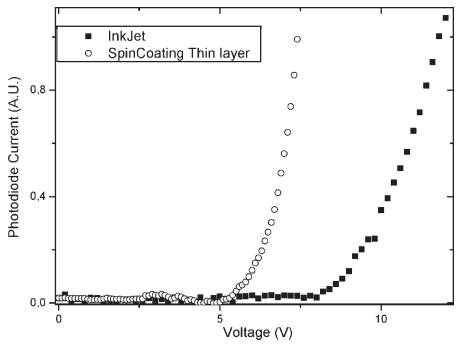

Figure 4.
Optical thresholds evaluation from EL-V plots.

Looking at the electroluminescence plots reported in Figure 4, the optical threshold values for each device correspond to the electrical threshold values identified in Figure 3 (5.3 V for device with spin-coated PF6, 8.1 V for OLED with IJ printed HTL).

Moreover, the IJ-printed device luminance slope is slightly different from those of the spin-coated device. These differences probably can be justified by the already cited differences in the distribution of trap energy levels that gives rise to non-radiative recombination processes or more probably in terms of the printed film thickness variability; indeed, the OLED optical turn-on is the resultant of the partial optical switches from device sections with different thickness.

Conclusion

In this work we employed IJP technology to fabricate OLEDs on flexible substrate and studied how the deposition method affected the device performances. We manufactured double-layer structures ink-jet printing only the hole-transporting layer and evaporating all the other layers. Moreover, in order to compare this technology with the traditional spin-coating technique we prepared the same electroluminescent structures by replacing the ink-jet printed polymer with a spin-coated film employing the same

solution used as ink. The results showed same differences in current density and optical behaviours between the devices fabricated by means these two technologies which can be justified in terms of both non-uniform thickness of the IJ-printed film and different trap distribution induced by impurity energy levels associated to each applied process. Moreover, in the comparison between these two technologies it is important to consider that their processes are carried out in different environmental conditions.

Despite the obtained results, further investigations are necessary to complete the analysis.

Acknowledgements: Support by TRIPODE project financed by the Ministero dell'Università e della Ricerca (MUR) is gratefully acknowledged.

[1] J. Bharathan, Y. Yang, *Applied Physics Letters* **1998**, *72*, 2660.
[2] T. R. Hebner, C. C. Wu, D. Marcy, M. H. Lu, J. C. Sturm, *Applied Physics Letters* **1998**, *72*, 519.
[3] Y. Yang, S.-C. Chang, K. Bharathan, J. Liu, *Journal of Materials Science: Materials in Electronics* **2000**, *11*, 89.
[4] J. H. Burroughes, D. D. C. Bradley, A. R. Brown, R. N. Marks, K. Mackay, R. H. Friend, P. L. Burns, A. B. Holmes, *Nature* **1990**, *347*, 539.
[5] C. W. Tang, S. A. VanSlyke, C. H. Chen, *Journal of Applied Physics* **1989**, *65*, 3610.
[6] D. Braun, A. J. Heeger, *Applied Physics Letters* **1991**, *58*, 1982.
[7] R. D. Deegan, O. Bakajin, T. F. Dupont, G. Huber, S. R. Nagel, T. A. Witten, *Nature* **1997**, *389*, 827.
[8] R. D. Deegan, *Physical Review E* **2000**, *61*, 475.
[9] E. Tekin, E. Holder, D. Kozodaev, U. S. Shubert, *Advanced Functional Materials* **2007**, *17*, 277.
[10] A. F. Ozdemir, A. Gok, A. Turut, *Thin Solid Films* **2007**, *515*, 7253.
[11] J. Sworakowski, G. F. Leal Ferreira, *Journal of Physics D: Applied Physics* **1984**, *17*, 135.

